Opposite Stereoselective Resistance to Digestion by Phosphodiesterases I and II of Benzo[*a*]pyrene Diol Epoxide-Modified Oligonucleotide Adducts†

Bing Mao,‡ Bin Li,‡ Shantu Amin,§ Monique Cosman,‡,‖ and Nicholas E. Geacintov*,‡

Chemistry Department, New York University, New York, New York 10003, and Naylor Dana Institute for Disease Prevention, American Health Foundation, Valhalla, New York 10595

Received April 1, 1993; Revised Manuscript Received August 20, 1993®

ABSTRACT: The deoxyribooligonucleotide 5′-d(CTCACATGTACACTCT) was reacted separately with the chiral diol epoxide isomers 7β,8α-dihydroxy-9α,10α-epoxy-7,8,9,10-tetrahydrobenzo[*a*]pyrene [(+)-*anti*-BPDE)] and 7α,8β-dihydroxy-9β,10β-epoxy-7,8,9,10-tetrahydrobenzo[*a*]pyrene [(−)-*anti*-BPDE)], to produce the modified oligonucleotides 5′-d(CTCACATG^{BPDE}TACACTCT). Adducts in which either (+)-*anti*-BPDE or (−)-*anti*-BPDE are covalently bound via their C10 positions by *trans* addition to the exocyclic amino group of the single G residues were isolated and purified by HPLC methods. Snake venom phosphodiesterase (SVPD, phosphodiesterase I), which hydrolyzes DNA from the 3′-OH terminus to the 5′-end, digests the (+)-*trans*-*anti*-BPDE–oligonucleotide adducts at a significantly faster rate than that of the sterically different (−)-*trans*-*anti*-BPDE–oligonucleotide adducts. However, using spleen phosphodiesterase (SPD, phosphodiesterase II), which hydrolyzes DNA in the 5′ → 3′ direction, the opposite stereoselective resistance to digestion is observed. Using shorter BPDE-modified oligonucleotides as standards, the enzyme stall sites have been defined by gel electrophoresis methods; the most digestion-resistant phosphodiester linkage is the 5′-d(...T-G*...)-3′ bond in the case of (+)-*trans*-BPDE-modified oligonucleotide adducts for both enzymes, SVPD and SPD (the starred G denotes the site of BPDE modification). In the case of the (−)-*trans*-BPDE-modified oligonucleotide adducts, the phosphodiester bond on the 3′-side of the modified G [5′-d(...G*-T...)-3′] is most resistant to digestion by both enzymes. It is concluded that in *single-stranded* oligonucleotides the pyrenyl residues point toward the 5′-end, while in (−)-*trans* adducts they point toward the 3′-end of the modified strands, paralleling the orientations recently found by 2D NMR techniques in analogous (+)-*trans*- and (−)-*trans*-BPDE–oligonucleotide *duplexes* [de los Santos et al. (1992) *Biochemistry 31*, 5245–5252]. Overall rates of enzyme digestion are more hindered whenever the bulky pyrenyl residue points in a direction opposing the progress of hydrolysis and are more facile when the pyrenyl ring points along the direction (3′ → 5′ or 5′ → 3′) of exonuclease digestion. Identification of exonuclease digestion stall sites in single-stranded oligonucleotides modified with bulky adducts may prove useful for deducing the orientations of these covalently bound residues relative to the modified base and the 5′–3′ strand polarity.

The effects of chirality are of critical importance in determining the nature of the interactions and chemical binding of mutagenic and carcinogenic diol epoxide metabolites of environmental polycyclic aromatic hydrocarbons (PAH) with DNA, and the biological consequences attributed to the covalent nucleic acid lesions (adducts) that are formed (Conney, 1982; Singer & Grunberger, 1983). The exonucleases snake venom phosphodiesterase (SVPD)[1] or spleen phosphodiesterase (SPD) (phosphodiesterases I and II, respectively) are routinely employed to degrade PAH metabolite–DNA adducts to the nucleotide or nucleoside levels for the identification and characterization of the lesions [see, for example, Gupta et al. (1982), Cheng et al. (1989), and Cheh et al. (1990)]. The resistance to exonuclease digestion of DNA adducts with covalently bound derivatives of 7,12-dimethylbenz[*a*]anthracene (Dipple & Pigott, 1987; Stezowski et al., 1987), benz[*a*]anthracene, benzo[*c*]phenanthrene (Cheh et al., 1990), and benzo[*a*]pyrene (Cosman, 1991; Osborne, 1993) has been reported. The focus of our interest is on the stereochemical aspects of this phenomenon using adducts derived from the binding of chiral benzo[*a*]pyrene diol epoxide derivatives to DNA.

The basic characteristics of SVPD and SPD have been reviewed (Laskowski, 1971; Bernardi & Bernardi, 1971). The

† This work was supported by the Office of Health and Environmental Research, Department of Energy, Grant DE-FGO2-86ER60405. The oligonucleotide and adduct synthesis facilities are supported by Grants CA 20851 from the U.S. Public Health Service, Department of Health and Human Services, awarded by the National Cancer Institute. The synthesis of the *anti*-BPDE enantiomers at the American Health Foundation was supported by PHS/DHHS/NIH/NCI Contract NO1-CP-21115 and Grant CA 57226-01.

* Corresponding author.

‡ New York University.

§ American Health Foundation.

‖ Present address: Cellular Biochemistry and Biophysics Program, Memorial Sloan-Kettering Cancer Center, New York, NY 10021.

® Abstract published in *Advance ACS Abstracts*, October 15, 1993.

[1] Abbreviations: SVPD, snake venom phosphodiesterase (phosphodiesterase I); SPD, spleen phosphodiesterase (phosphodiesterase II); (+)-*anti*-BPDE, 7β,8α-dihydroxy-9α,10α-epoxy-7,8,9,10-tetrahydrobenzo[*a*]pyrene; (−)-*anti*-BPDE, 7α,8β-dihydroxy-9β,10β-epoxy-7,8,9,10-tetrahydrobenzo[*a*]pyrene; (+)- or (−)-*trans*-*anti*-BPDE-N^2-dG, mononucleoside adducts derived from the covalent binding by *trans* addition of either of the two *anti*-BPDE enantiomers via their C10 positions to the exocyclic (N^2) amino groups of 2′-deoxyguanosine (dG); (+)- or (−)-*trans*-oligonucleotide adduct, d(CTCACATG^{BPDE}TACACTCT) with analogous stereochemical characteristics as the corresponding (+)- or (−)-*trans*-*anti*-BPDE-N^2-dG mononucleoside adducts at the modified dG residues.

0006-2960/93/0432-11785$04.00/0

enzyme SVPD successively hydrolyzes 5′-mononucleotides from deoxyribooligonucleotides with free 3′-OH groups, and thus digestion of the DNA proceeds in the 3′ → 5′ direction. In contrast, SPD requires 5′-OH termini, and digestion proceeds in the opposite direction (5′ → 3′). Both SVPD (Nossal & Singer, 1968; Brody et al., 1986) and SPD (Thomas & Olivera, 1978) are nonprocessive enzymes. While the exact mechanisms of hydrolysis are not yet understood, these enzymes are known to bind to the DNA substrates and to catalyze partial hydrolysis, followed by dissociation of the complexes, the subsequent binding of the enzyme to other DNA molecules, and the repetition of the hydrolysis cycles. In contrast, processive exonucleases bind to one single DNA molecule and hydrolysis continues until the degraded oligonucleotides are only 10–12 bases long (Brody, 1991).

In living cells, benzo[*a*]pyrene is metabolized to many different oxygenated derivatives which include four highly reactive and biologically active bay-region diol epoxide derivatives (Conney, 1982; Singer & Grunberger, 1983). Particularly striking are the differences in the biological activities of the two enantiomers 7β,8α-dihydroxy-9α,10α-epoxy-7,8,9,10-tetrahydrobenzo[*a*]pyrene [(+)-*anti*-BPDE] and 7α,8β-dihydroxy-9β,10β-epoxy-7,8,9,10-tetrahydrobenzo-[*a*]pyrene [(−)-*anti*-BPDE]. The (+)-*anti*-BPDE isomer is more mutagenic than (−)-*anti*-BPDE in mammalian cell systems, while in some bacterial strains the (−)-enantiomer is more active (Wood et al., 1977; Brookes & Osborne, 1982; Stevens et al., 1985); furthermore, (+)-*anti*-BPDE is highly tumorigenic, while the (−)-enantiomer is not (Buening et al., 1978; Slaga et al., 1979). The reverse ordering of the relative mutagenicities of (+)-*anti*-BPDE and (−)-*anti*-BPDE in mammalian and in bacterial cell systems suggests that the processing of adducts by cellular enzymes must be quite different in these two types of mutagenesis test systems (Stevens et al. , 1985).

In this work, we have covalently modified the 16-mer d(CTCACATGTACACTCT) by *trans* addition (Cheng et al., 1989) at the exocyclic amino group of the single guanosyl moiety with (+)-*anti*-BPDE and (−)-*anti*-BPDE. Using high-resolution gel electrophoresis methods, we show that the relative efficiencies of digestion of the modified single-stranded oligonucleotides by SVPD and SPD are remarkably different and depend on the adduct stereochemistry relative to the 3′ → 5′ (SVPD) or 5′ → 3′ (SPD) directions of enzyme digestion. A simple model accounting for the stereoselective resistance to enzyme digestion in terms of the orientations of the pyrenyl residues relative to the 5′–3′ strand polarity is proposed. Our findings suggest that exonuclease enzyme digestion methods can be useful in defining bulky adduct orientations in site-specifically modified single-stranded DNA.

MATERIALS AND METHODS

Synthesis of anti-BPDE Enantiomers. Benzo[*a*]pyrene-7,8-diol was synthesized as described previously (Yagi et al., 1977) and was resolved into the *R*,*R* and *S*,*S*-enantiomers by chiral stationary-phase HPLC according to published methods (Yang et al., 1984; Weems et al., 1986). The resulting dihydrodiols were oxidized to the corresponding diol epoxides (+)- and (−)-*anti*-BPDE by *m*-chloroperbenzoic acid (Yagi et al., 1977).

Synthesis and Purification of Oligonucleotides. The oligonucleotide 5′-d(CTCACATGTACACTCT) was synthesized on a Cyclone DNA synthesizer (Biosearch, Inc., San Rafael, CA), deprotected by routine phosphoramidite procedures (Caruthers, 1982), and purified as described earlier (Cosman et al., 1990). The oligonucleotides 5′-d(CTCACATGT) and 5′-d(TGTACACTCT) were purchased from The Midland Certified Reagent Co. (Midland, TX).

Modification and Purification of anti-BPDE Adducts. The oligonucleotide d(CTCACATGTACACTCT) was modified covalently with (+)-*anti*-BPDE and (−)-*anti*-BPDE as described earlier (Cosman, et al, 1990). The *anti*-BPDE-N^2-dG oligonucleotide adducts were separated by HPLC employing a 10 × 250 mm Hypersil-ODS column (Keystone Scientific, Inc., Bellefonte, PA) and a 0–90% linear gradient of a methanol/20 mM sodium phosphate buffer solution (pH 7.0) in 60 min with a flow rate of 3 mL/min. Both UV and fluorescence detectors were used. The wavelength was 254 nm for UV absorption detection, while for fluorescence detection, the excitation wavelength was 344 nm and the emission wavelength was 400 nm. The oligonucleotides 5′-d(CTCACATGT) and 5′-d(TGTACACTCT) were modified covalently with racemic BPDE. Stereospecific 5′-d(TG^{BPDE}-TACACTCT) adducts were separated by HPLC using a 0–35% linear gradient of a methanol/20 mM sodium phosphate buffer solution (pH 7.0) in 60 min with a flow rate of 3 mL /min. The stereochemically different adducts 5′-d(CTCACATG^{BPDE}T) were first separated from the unmodified oligonucleotide using the same procedure, and the adduct fraction was collected, evaporated to dryness, and redissolved in water. The adducts were then subjected to further HPLC separation with a 25–35% linear gradient of methanol and phosphate buffer in 60 min, with a flow rate of 1 mL/ min using a Microsorb-MV C-18, 4.5 × 250 mm, 5-μm analytical column (Rainin Instrument, Inc., Woburn, MA). The stereochemical characteristics of these adducts were also determined by enzymatically digesting the BPDE-modified oligonucleotides to the BPDE-N^2-dG mononucleoside levels, by coelution of the latter with BPDE-N^2-dG adduct standards (Cheng et al., 1989), and via the CD spectra of the individual BPDE–mononucleoside adducts (Cosman et al., 1990). Both the (+)- and (−)-*trans*-*anti*-BPDE-N^2-dG-modified oligonucleotide 9- or 10-mers were used as size markers in gel electrophoresis experiments.

Circular Dichroism (CD) Spectra. The CD spectra were determined with a home-built CD system which was calibrated with a *d*-camphorsulfonic acid solution (Cassim, 1969); the magnitude of the CD signal is reported in terms of molar ellipticities for an optical path length of 1 cm (Cosman, 1990, Cosman, 1991), and in terms of mdeg/au (Cheng et al., 1989; Weems & Yang, 1989), where au is the absorbance at the 350-nm maximum of the BPDE–oligonucleotide adducts. The molar concentrations of BPDE residues (or modified strands) were calculated by using a molar extinction coefficient of 29 500 M^{-1} cm^{-1} at 350 nm (Cosman et al., 1990). Absorption spectra were determined with an Aviv Model 14 DS UV–vis spectrophotometer (Aviv Associates, Lakewood, NJ).

Phosphorylation and Strand Purification. The oligonucleotides d(CTCACATGTACACTCT), d(CTCACATGT), and the corresponding *trans*-*anti*-BPDE-N^2-dG oligonucleotide adducts (50 ng of each) were labeled at their 5′-termini by using T4 polynucleotide kinase (Pharmacia, Piscataway, NJ) and [γ-^{32}P]ATP (New England Nuclear, Boston, MA). Labeling at the 3′-termini was achieved by first forming an overhanging duplex d(CTCACATG^{BPDE}TACACTCT)·d(GAGAGTGTACATGTGA) and d(TGTACACTCT)·d(GAGAGTGTACA), and then by using the Klenow fragment of *Escherichia coli* DNA polymerase I (Pharmacia) and [α-^{32}P]CTP (New England Nuclear, Boston, MA) to

extend the 3′-termini. All labeled samples were heated for 2 min at 90 °C, cooled to 0 °C, and loaded on a 20% denaturing polyacrylamide gel. The gel was operated at 2500 V for 2 h at 45 °C and exposed briefly to Kodak X-OMAT AR film (Eastman Kodak Co., Rochester, NY); the bands corresponding to the 16-mer were cut out and soaked overnight at 37 °C in 0.3 mL of buffer (0.5 M ammonium acetate, 10 mM magnesium diacetate). The extracted solutions were passed through a Bio-Gel P-6 spin column (Bio-Rad, Melville, NY) for desalting. The samples were lyophilized and redissolved in the appropriate reaction buffers.

Snake Venom Phosphodiesterase Digestion. The SVPD (Pharmacia) digestion was carried out at room temperature in 60 μL of solution containing 5′-termini-labeled unmodified or (+)- or (−)-*trans*-BPDE-N²-dG-modified oligonucleotides d(CTCACATGTACACTCT) or d(CTCACATG^{BPDE}TACACTCT), 0.2 unit of SVPD, 1 μg of unlabeled adduct, and reaction buffer (15 mM $MgCl_2$, 0.11 M Tris, pH 8.9). Unlabeled oligonucleotide was added in order to ensure identical concentrations, and thus reproducibility, in different experiments. Ten microliters of the reaction mixture was taken out after different time intervals, and the digestion was terminated by addition of EDTA (10 mM final concentration).

Spleen Phosphodiesterase Digestion. Digestion with this enzyme (Boehringer-Mannheim, Indianapolis, IN) was performed at room temperature in 60 μL of solution which contained 3′-termini labeled single-strand (+)- or (−)- *trans*-oligonucleotide adducts, 0.1 unit of SPD, 1 μg of unlabeled adduct, and the reaction buffer (0.25 M sodium succinate, pH 6.5); 10-μL aliquots of the reaction mixtures were sampled at different time periods after adding 10 μL of the stop solution (0.0059 M uranyl acetate in 2.5% perchloric acid) to these aliquots.

Gel Electrophoresis. Seven-microliter aliquots of the digestion mixtures in loading buffer (98% formamide solution) were placed in the wells of denaturing gels (20% acrylamide, 19:1 monomer/bis ratio, 7 M urea) for 2 h at 2500 V and 45 °C using a Poker-Face II Model SE 1600 gel electrophoresis apparatus 40 cm long (Hoefer Scientific Instruments, San Francisco, CA). The buffer system contained 89 mM Tris, 89 mM borate, pH 8.9, and 2 mM EDTA (TBE buffer). The gel was dried immediately on a vacuum drying apparatus (Hoefer Scientific Instruments) and was exposed to X-ray film at room temperature.

Enzyme Digestion of BPDE-Modified Oligonucleotides to BPDE–dG Mononucleoside Adducts, and HPLC Analysis. The unmodified and modified oligonucleotides were hydrolyzed to deoxyribonucleosides using SVPD and bacterial alkaline phosphatase (McLaughlin & Piel, 1984). Approximately 2 μg of sample, 3 units of SVPD, and 3 units of bacterial alkaline phosphatase were added to 200 μL of a 100 mM Tris-HCl, pH 8.8, and 20 mM $MgCl_2$ buffer solution and allowed to react overnight at 37 °C. The resulting digests were analyzed by HPLC using a Microsorb-MV C-18, 4.5 × 250 mm, 5-μm analytical column (Rainin Instrument, Inc., Woburn, MA) with a linear 0–100% methanol/20 mM sodium phosphate buffer (pH 7.0) gradient in 60 min and a flow rate of 1 mL/min. The *anti*-BPDE-N²-dG adduct fractions were collected, and their elution times and CD spectra were compared with those of BPDE-N²-dG standards; the latter were prepared as described by Cheng et al. (1989).

RESULTS

Separation of (+)- and (−)-anti-BPDE–Oligonucleotide Adducts. High-performance liquid chromatography elution profiles of (+)-*anti*-BPDE–oligonucleotide and (−)-*anti*-BPDE–oligonucleotide reaction mixtures are shown in Figure 1, panels A and B, respectively. Three different elution maxima, characterized by their absorbances at 254 nm, are evident. Absorbance peaks A1 and B1 at 18 min are due to the unmodified oligonucleotide 5′-d(CTCACATGTACACTCT), and as expected, there is no fluorescence associated with these elution maxima. The next two eluates (A2, A3 and B2, B3) contain (+)- and (−)-*anti*-BPDE–oligonucleotide 5′-d(CTCACATG^{BPDE}TACACTCT) adducts, respectively, and are characterized by fluorescence emission upon excitation at 350 nm (upper, thin lines in Figure 1, panels and B). The corresponding fluorescence excitation and emission spectra (data not shown) are characteristic of the pyrenyl residue (Geacintov et al., 1991). The combined yields of (+)- and (−)-*anti*-BPDE–oligonucleotide adducts amount to about 15–20% on the basis of the oligonucleotide strand concentration.

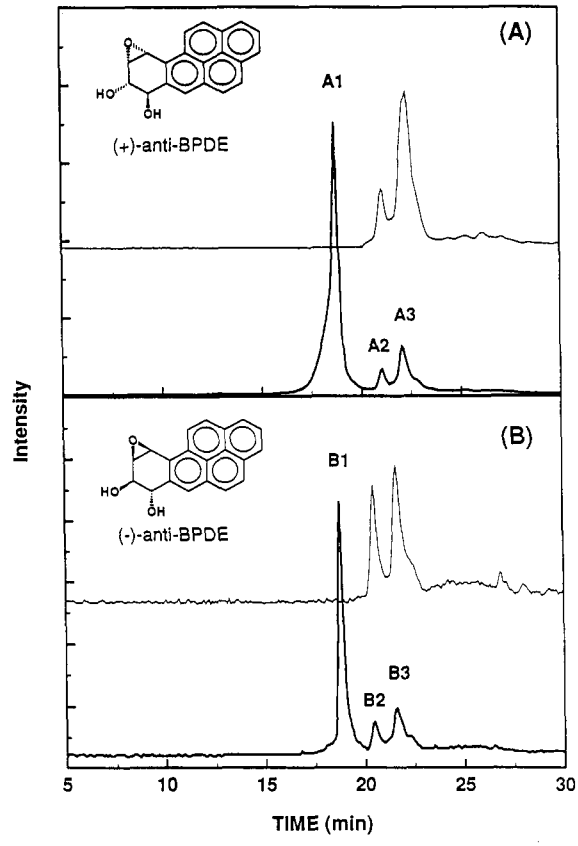

FIGURE 1: HPLC elution profile of (A) (+)-*anti*-BPDE–d(CTCACATGTACACTCT) reaction mixture and (B) (−)-*anti*-BPDE–d(CTCACATGTACACTCT) reaction mixture. Peaks A1 and B1: unmodified oligonucleotides; peak A3: (+)-*trans-anti*-BPDE-N²-dG oligonucleotide adduct; peak B2: (−)-*trans-anti*-BPDE-N²-dG oligonucleotide adduct; peaks A2 and B3 are *cis-anti*-BPDE-N²-dG oligonucleotide adducts. Heavy lines (bottom traces): detection by absorbance at 254 nm; thin lines (upper traces): detection by fluorescence (excitation 350 nm, emission viewed at 400 nm).

Determination of BPDE-N²-dG Oligonucleotide Adduct Stereochemistry. Each of the four eluates (A2, A3, B2, and B3) were subjected to digestion using the enzymes SVPD and bacterial alkaline phosphatase to obtain (+)- or (−)-*anti*-BPDE–N²-deoxyguanosine mononucleoside adducts as described recently (Cheng et al.,1989; Cosman et al., 1990; Geacintov et al., 1991). The HPLC elution profiles of enzyme digests of the unmodified oligonucleotide fractions A1 (or B1) and modified oligonucleotide fractions A3 and B2 (all defined in Figure 2) are shown in Figure 2, panels A, B, and C, respectively. In Figure 2A, elution peaks due to each of

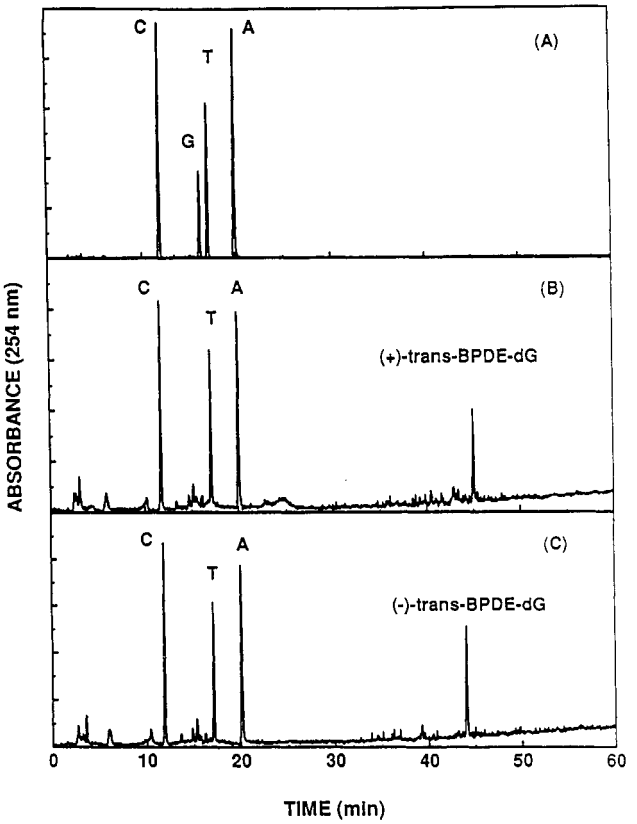

FIGURE 2: HPLC chromatograms showing the enzyme digests (3 units each of SVPD and bacterial alkaline phosphatase in a 200-μL solution) of (A) unmodified oligonucleotide, (B) (+)-*trans*-BPDE–d(CTCACATG^{BPDE}TACACTCT) adduct (HPLC elution peak A3 in Figure 1A), and (C) (–)-*trans*-BPDE–d(CTCACATG^{BPDE}TACACTCT) adduct (HPLC elution peak B2 in Figure 1B). The eluates with retention times in the vicinity of 45 min are *trans*-BPDE-N^2-dG mononucleoside adducts; the CD spectra of these fractions are shown in Figure 3.

the four nucleosides are observed; however, in Figure 2B,C, similar elution maxima are observed, except that the dG peaks are missing (the small residual maxima near 16 min in Figure 2B,C, are due to enzyme solution components). Instead, eluates containing single (+)- or (–)-*anti*-BPDE-N^2-dG adducts are observed which coelute (data not shown) with either a *trans*-(+)-*anti*-BPDE-N^2-dG adduct standard (enzyme digest of eluate A3) or a *trans*-(–)-*anti*-BPDE-N^2-dG adduct standard (enzyme digest of eluate B2). Furthermore, the CD spectrum of the enzyme digest of eluate A3 is the same as that of the authentic *trans*-(+)-*anti*-BPDE-N^2-dG adduct, while the CD spectrum of the enzyme digest of eluate B2 coincides with that of the authentic *trans*-(–)-*anti*-BPDE-N^2-dG adduct (Cheng et al, 1989); the CD spectra of the enzyme digests of fractions A3 and B2 (the HPLC elution fractions at 44–45 min, Figure 2B,C), shown in Figure 3, are mirror images of one another, as expected for BPDE-dG adducts derived from the binding of the chiral (+)- and (–)-*anti*-BPDE isomers to dG (Cheng et al., 1989). In summary, eluates A3 and B2 contain the deoxyoligonucleotide 5′-d(CTCACATG^{BPDE}TACACTCT) in which the single guanosine residues are modified covalently via *trans* addition of (+)-*anti*-BPDE and (–)-*anti*-BPDE, respectively, to the exocyclic amino group of the single dG bases; these will be designated as the (+)-*trans*- and(–)-*trans*-oligonucleotide adducts, respectively. Eluates A2 and B3 contain the corresponding (+)-*cis*- and (–)-*cis*-oligonucleotide adducts (data not shown), and their properties were not further investigated here.

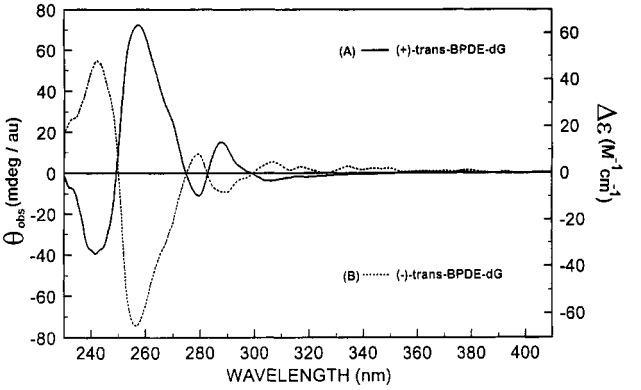

FIGURE 3: Circular dichroism spectra of *trans*-BPDE-N^2-dG mononucleoside adduct obtained from enzyme digests of *trans-anti*-BPDE–oligonucleotide adducts (A) derived from the covalent binding of (+)-*anti*-BPDE (HPLC fraction A3 in Figure 1A) and (B) derived from the covalent binding of (–)-*anti*-BPDE (HPLC fraction B2 in Figure 1B). The vertical scales are expressed in terms of mdeg/au (where au denotes the absorbance units at the absorption peak of 345 nm) (left-hand scale) and in terms of molar ellipticities (right-hand scale).

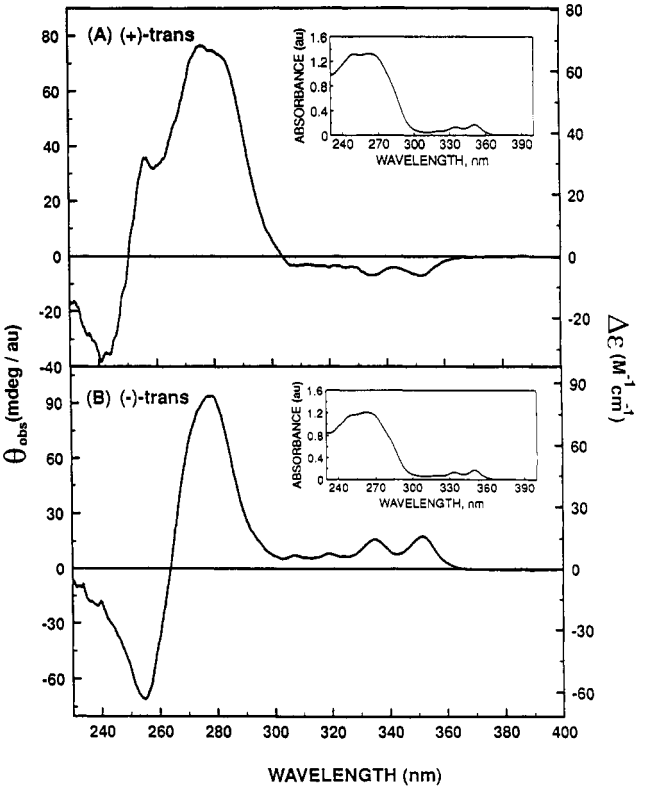

FIGURE 4: Circular dichroism spectra of *trans-anti*-BPDE–oligonucleotide adducts. (A) (+)-*trans-anti*-BPDE–oligonucleotide adduct (HPLC fraction A3 in Figure 1A) and (B) (–)-*trans-anti*-BPDE-oligonucleotide adduct (HPLC fraction B2 in Figure 1B); the vertical scale is expressed in terms of mdeg/au (au denotes the absorbance units at the absorption peak of 350 nm) (left-hand scale) and in terms of molar ellipticities (right-hand scale). The respective absorption spectra are shown in the insets (~7 μM strand concentration).

Spectroscopic Characteristics of trans-Oligonucleotide Adducts. The absorption and CD spectra of the (+)-*trans*- and (–)-*trans*-oligonucleotide adducts are compared to one another in Figure 4. The absorption spectra are very similar for both types of adducts, with maxima at 248, 334, and 350 nm attributable to the pyrene-like aromatic residue (Cosman et al., 1990; Geacintov et al., 1991). Above 300 nm, the CD spectra resemble the absorption spectra in shape, with the signs of the ellipticities being either positive [(–)-*trans*-adducts]

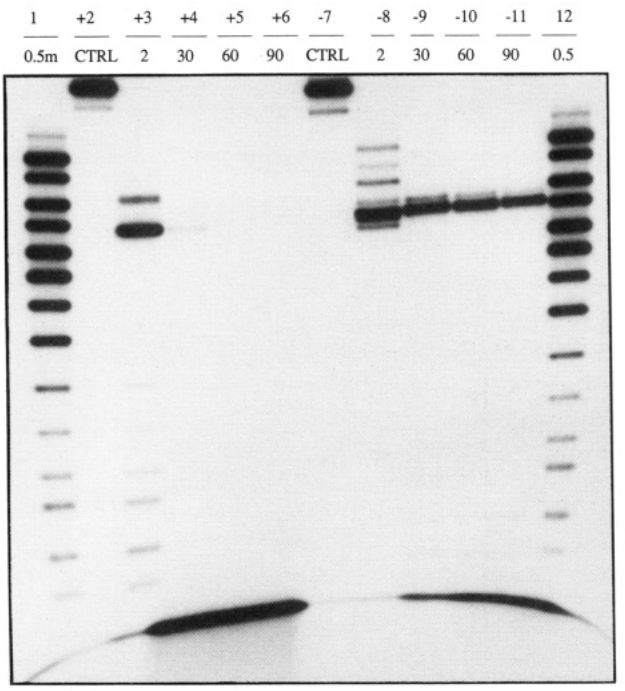

FIGURE 5: Gel electrophoresis of SVPD digestion mixture (0.2 unit in 60 μL) of *trans-anti*-BPDE–d(CTCACATG^{BPDE}TACACTCT) adducts. Lanes 1 and 12: unmodified oligonucleotide digested for 0.5 min. Lanes +2 and –7: controls, undigested (+)-*trans-anti*-BPDE– and (–)-*trans-anti*-BPDE–oligonucleotide adducts, respectively. Lanes +3 to +6: (+)-*trans-anti*-BPDE–oligonucleotide adduct digested for 2, 30, 60, and 90 min, respectively. Lanes –8 to –11: (–)-*trans-anti*-BPDE–oligonucleotide adduct digested for 2, 30, 60, and 90 min, respectively. The + and – signs in front of the lane designations denote oligonucleotide adducts derived from (+)- and (–)-*anti*-BPDE, respectively.

FIGURE 6: Gel electrophoresis of SPD digestion mixture (0.1 unit in 60 μL) of *trans-anti*-BPDE (CTCACATG^{BPDE}TACACTCT) oligonucleotide adducts. Lanes 1 and –12: unmodified oligonucleotide (CTCACATGTACACTCT) digested for 1 min. Lanes +2 and –7: controls, undigested (+)-*trans-anti*-BPDE– and (–)-*trans-anti*-BPDE–oligonucleotide adducts, respectively. Lanes +3 to +6: (+)-*trans-anti*-BPDE oligonucleotide adduct digested for 1, 5, 120, and 240 min, respectively. Lanes –8 to –11: (–)-*trans-anti*-BPDE–oligonucleotide adduct digested for 1, 5, 120, and 240 min, respectively.

or negative [(+)-*trans*-adducts]. The characteristics of these CD spectra are attributed to the asymmetry of the environment of the pyrenyl residues (induced CD effects). Below 300 nm, the CD spectra are complex because of the superposition of the coupled exciton CD spectra (Harada & Nakanishi, 1983) of the BPDE-N2-dG moieties (Figure 3) and the nucleic acid residues.

SVPD Digestion (3′ → 5′) of trans-Oligonucleotide Adducts. Electrophoresis gel patterns of solutions of the unmodified 16-mer 5′-d(CTCACATGTACACTCT) and the (+)-*trans*- and (–)-*trans*-oligonucleotide adducts subjected to digestion with SVPD for various digestion times are shown in Figure 5.

Digestion of the unmodified oligonucleotide with SVPD for only 30 s yields a series of 16 bands of varying intensities (Figure 5, lane 1); the uppermost, faint band is attributed to a small amount of residual undigested 16-mer, while the higher-mobility fragments are due to progressively shorter fragments (from top to bottom). The dark bands in lanes +2 and –7 indicate that the mobilities of the undigested (+)- and (–)-*trans*-oligonucleotide adducts (controls) are considerably slower than that of the unmodified oligonucleotide, as described earlier (Mao et al., 1992); the fainter bands in lanes +2 and –7 just below the dark bands are probably oligonucleotide adduct decomposition products and were not identified. After 2 min of digestion with SVPD, a prominent undigested band (lane +3) is observed at approximately the same level as the fifth band from the top in lane 1; a series of 7 lower molecular weight fragments is also present; these bands coincide in position with bands 10–16 (counted from the top) of the shorter oligonucleotide fragments arising from the digestion of the unmodified oligomer (lane 1). However, upon digestion of the (+)-*trans*-oligonucleotide adducts for longer times (lanes +4 to +6), it is evident that degradation is complete after 60–90 min. In the case of the (–)-*trans*-oligonucleotide adducts (lanes –7 to –11), on the other hand, it is evident that digestion is partially blocked at a specific site, since dark single bands (which comigrate with the fifth band from the top of the partially digested unmodified oligonucleotide, lane 12) are evident after 2, 30, 60, and 90 min of digestion with SVPD (Figure 5).

Evidently, digestion by SVPD is significantly slowed in the case of both (+)-and (–)-*trans-anti*-BPDE adducted 16-mers, but this effect is much more strongly pronounced in the case of the (–)-*trans-anti*-BPDE–oligonucleotide adduct. This difference is particularly striking after 90 min of digestion (lanes +6 and –11). We conclude from these observations that both types of adducted bulky BPDE residues inhibit the progress of digestion, but that the (–)-*trans-anti*-BPDE–16-mer adduct is more resistant to digestion by the exonuclease snake venom phosphodiesterase I than the corresponding (+)-*trans-anti*-BPDE–16-mer adduct.

SPD Digestion (5′ → 3′) of trans-Oligonucleotide Adducts. Results of the digestion of (+)-*trans* and (–)-*trans*-oligonucleotide adducts by SPD are depicted in the photograph of a typical electrophoretic gel (Figure 6). Lanes 1 and 12 represent a ladder of fragments of different sizes obtained from the digestion of the unmodified 17-mer by SPD for 1 min (an extra dC is incorporated at the 3′-end in the 3′-labeling reaction); digestion is incomplete within this short time interval, and only 11 bands are visible in this case. The bands due to

the undigested (+)-*trans*- and (–)-*trans*-oligonucleotide adduct controls are shown in lanes +2 and –7, respectively. Lanes +3 to + 6, and lanes –8 to –11, depict the products obtained after digestion of (+)-*trans*- and (–)-*trans*-oligonucleotide adducts, respectively, for varying periods of time (1–240 min). The results are opposite to those observed in the case of SVPD: the progress of digestion by SPD is significantly slower in the case of the (+)-*trans* adduct than in the case of the (–)-*trans*-oligonucleotide adduct. After a 4-h period, the digestion of the (–)-*trans*-oligonucleotide adduct is complete (lane –11). In the case of the (+)-*trans* adduct, however, a prominent band due to an undigested fragment is still visible near the top of the gel (lane +6); this band comigrates with the fourth band from the top in lane 1 which arises from the partial digestion of the unmodified oligonucleotide. Thus, the (+)-*trans*-BPDE–16-mer adduct is more resistant to digestion by SPD than the corresponding (–)-*trans*-BPDE–oligonucleotide adduct.

Determinations of Enzyme Stall Sites. The oligonucleotide fragments that are most resistant to digestion by SVPD appear to be similar in size for the (+)-*trans*- and (–)-*trans* adduct (Figure 5, lanes +3 and –8 to –11, respectively). In the case of SPD, the sizes of the digestion-resistant (+)-*trans*- and (–)-*trans*-oligonucleotide fragments appear to be different (compare, for example, lanes +3 to +6 with lane –9, Figure 6). However, attempts to relate the size of the fragments to one another are difficult because of the intrinsically slower mobilities of (+)-BPDE-modified, as compared to (–)-BPDE-modified, oligonucleotides [Shibutani et al. (1993) and compare, for example, lanes +2 and –7 in Figure 6]; Shorter fragments bearing BPDE-N^2-dG residues exhibit larger differences in mobilities (Mao et al., 1992). Comparisons of the sizes of the enzyme digest fragments with those derived from Maxam–Gilbert sequencing reactions (Maxam & Gilbert, 1980) are not entirely suitable for precise length determinations; the Maxam–Gilbert fragments have 3′-phosphate residues, while the enzyme digest fragments have 3′-OH (or 5′-OH) ends.

In order to overcome these problems and to determine the sites of the most prominent enzyme stall sites (the darkest bands in lanes +3 and –11, Figure 5, and lanes +6 and –9, Figure 6), we compared the electrophoresis patterns of the enzyme digests of the BPDE-modified 16-mer oligonucleotides with standards obtained by covalently modifying shorter oligonucleotide fragments (9–10 bases long) with BPDE. The labeled fragments synthesized for identifying SVPD enzyme stall sites were derived from the binding of (+)-BPDE and (–)-BPDE to the exocyclic amino group of the single G residue in d(CTCACATGT) and are labeled **+I** and **–I**, respectively, as follows:

(+)-*trans*-5′-d([^{32}P]CTCACATG^{BPDE}T$_{OH}$)-3′

(fragment **+I**)

(–)-*trans*-5′-d([^{32}P]CTCACATG^{BPDE}T$_{OH}$)-3′

(fragment **–I**)

The labeled standard fragments synthesized for the identification of the SPD enzyme stall sites are

(+)-*trans*-5′-d($_{HO}$TG^{BPDE}TACACTCT[^{32}P]C$_{OH}$)-3′

(fragment **+II**)

(–)-*trans*-5′-d($_{HO}$TG^{BPDE}TACACTCT[^{32}P]C$_{OH}$)-3′

(fragment **–II**)

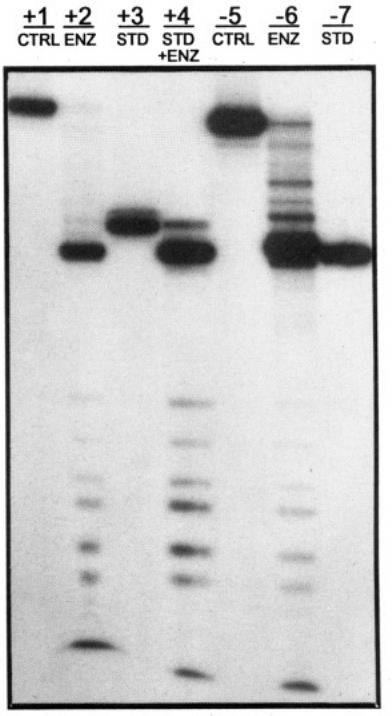

FIGURE 7: Determination of the SVPD enzyme digestion stall site and size of the corresponding BPDE-modified oligonucleotide fragments. Lanes +1 and –5, undigested controls: (+)-*trans*- and (–)-*trans*-BPDE-modified oligonucleotides 5′-d(CTCACATG^{BPDE}-TACACTCT), respectively. Lanes +2 and –6: partially SVPD enzyme-digested (2 min) modified oligonucleotides. Lanes +3 and –7: size markers, (+)- and (–)-*trans*-BPDE-modified d(CTCA-CATG^{BPDE}T) fragments, respectively. Lane +4: partial SVPD enzyme digest (2 min) of the size standard (+)-*trans*-d(CTCA-CATG^{BPDE}T) adduct fragment.

The subscripts indicate the presence of OH groups at the 3′- and 5′-ends of the oligonucleotide fragments.

SVPD Digestion. The results for 5′-end-labeled (+)-*trans*- and (–)-*trans*-16-mer adducts, relevant to the SVPD digestion experiments which proceed in the 3′ → 5′ direction, are shown in the photographs of the high-resolution gels in Figure 7. The bands due to the controls (undigested BPDE-modified 16-mers) are shown in lanes +1 and –5. The corresponding SVPD enzyme digests (2 min) showing the preferred enzyme stall fragments, are shown in lanes +2 and –6. The positions of the bands arising in the same gels from migrations of the sized standards **+I** (lane +3) and **–I** (lane –7) are also shown in Figure 7.

The most digestion-resistant fragment of the (–)-*trans*-BPDE-modified 16-mer (lane –6) comigrates with the standard fragment **–I** in lane –7 (the slight apparent difference in the mobilities of the bands in lanes –6 and –7 in Figure 7 is attributed to the slight systematic differences in the positions of even identical bands in the different lanes). The enzyme-resistant fragment is therefore identified as (–)-*trans*-d(CT-CACATG^{BPDE}T). We thus conclude that the phosphodiester bond between the (–)-BPDE-modified G and the T on the 3′-side of this lesion is most resistant to SVPD digestion.

However, in the case of the (+)-*trans*-16-mer SVPD enzyme digestion, the most resistant fragment migrates faster (lane +2, Figure 7) than the standard adduct fragment **+I** (lane +3). Therefore, the size of the enzyme-resistant fragment is *smaller* than that of the standard **+I**. However, if the fragment **+I** itself is subjected to SVPD enzyme digestion, a higher-mobility band (lane +4), which comigrates with the enzyme-resistant fragment derived from SVPD digestion of the modified 16-mer (lane +2), is observed; a lower-mobility and

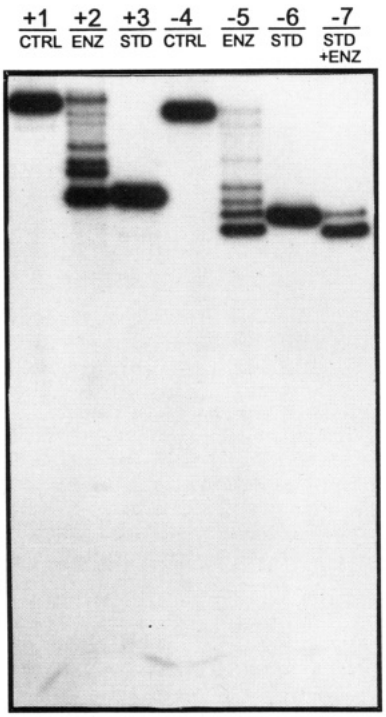

FIGURE 8: Determination of the SPD enzyme digestion stall site and size of the corresponding BPDE-modified oligonucleotide fragments. Lanes +1 and –4, undigested controls: (+)-*trans*- and (–)-*trans*-BPDE-modified oligonucleotides 5′-d(CTCACATG^{BPDE}TACACTCT), respectively. Lanes +2 and –5: partially SPD enzyme-digested (2 min) modified oligonucleotides. Lanes +3 and –6: size markers, (+)- and (–)-*trans*-BPDE-modified d(TG^{BPDE}TACACTCTC) fragments, respectively. Lane –7: partial SPD enzyme digest (2 min) of the size standard (+)-*trans*-d(TG^{BPDE}TACACTCTC) adduct fragment.

lower-intensity band due to undigested **+I** is also observed in lane +4. We therefore conclude that SVPD digestion removes the single T residue on the 3′-side of fragment **+I** to yield the SVPD-resistant fragment (+)-*trans*-d(CTCACATG^{BPDE}). The latter is therefore identified as the fragment which corresponds to the SVPD enzyme stall in the case of the (+)-*trans*-BPDE-modified 16-mer.

We note that the two SVPD-resistant fragments (+)-*trans*-5′-d(CTCACATG^{BPDE})-3′ and (–)-*trans*-adduct 5′-d(CTCACATG^{BPDE}T)-3′ exhibit nearly the same electrophoretic mobilities, even though the latter has an additional nucleotide. This is attributed to the intrinsically slower mobilities of (+)-BPDE-modified oligonucleotide adducts as compared to (–)-BPDE-modified oligonucleotides adducts (compare the mobilities of fragments **+I** and **–I,** lanes +3 and –7, respectively, in Figure 7).

SPD Digestion. The results for 3′-end-labeled (+)-*trans* and (–)-*trans* adducts, relevant to the SPD digestion experiments which proceed in the 3′ ← 5′ direction, are shown in the gels in Figure 8. The bands in lanes +1 and –4 pertain to the undigested (+)- and (–)-*trans*-oligonucleotides, respectively. Lanes +2 and –5 depict the bands obtained from the partial (2-min) digestion of these two modified 16-mers, respectively. The electrophoretic bands due to the two standards, fragments **+II** and **–II,** are shown in lanes +3 and –6, respectively.

In the case of SPD digestion of the (+)-*trans*-16-mer adduct, the fragment corresponding to the enzyme stall comigrates with fragment **+II**. Therefore, we identify this SPD digestion-resistant fragment as (+)-*trans*-d(TG^{BPDE}TACACTCTC).

However, in the case of the (–)-*trans*-16-mer oligonucleotide, the mobility of the most enzyme-resistant fragment (lane –5) is *faster* than that of fragment **–II** (lane –6). The next-slowest band in lane –5 does comigrate with standard **–II**, and thus has a T-residue on the 5′-side of the modified G. Digestion of the standard **–II** with SPD results in an enzyme digestion-resistant fragment that does comigrate with the SPD-resistant fragment derived from the digestion of the (–)-*trans*-16-mer oligonucleotide adduct (lanes –7 and –5, respectively). We therefore identify this fragment as (–)-*trans*-d(TG^{BPDE}-TACACTCTC).

The large differences in the sizes of the SPD enzyme-resistant fragments in Figure 6 (compare lanes +3 to +6 with lane –9, for example) are attributed to the slower mobilities of oligonucleotide fragments bearing (+)-BPDE residues as compared to the mobilities of fragments bearing (–)-BPDE residues (compare lanes +3 and –6 in Figure 8).

DISCUSSION

The resistance of several different covalent polycyclic aromatic hydrocarbon–deoxyadenosine adducts to digestion by phosphodiesterases has been previously reported. Stezowski et al. (1987) showed that 7,12-dimethylbenz[*a*]anthracene–N^6-deoxyadenosine lesions in oligonucleotides inhibit the activities of both SVPD and SPD. Dipple and Pigott (1987) reported that 7,12-dimethylbenz[*a*]anthracene diol epoxide–deoxyguanosine adducts are efficiently released by enzymatic hydrolysis with SVPD, but that the 7,12-dimethylbenz[*a*]-anthracene diol epoxide–deoxyadenosine adducts are significantly more resistant to digestion. Cheh et al. (1990) studied the relative efficiencies of digestion by SVPD and SPD of adenosine adducts derived from the binding of benz[*a*]-anthracene and benzo[*c*]phenanthrene bay-region diol epoxide to calf thymus DNA. Using HPLC methods for monitoring the release of diol epoxide–deoxyadenosine and –deoxyguanosine adducts, they found that guanosine adducts were efficiently released even at low enzyme activity levels, while the rate of release of adenosine adducts was stereoselective and depended on the stereoisomeric characteristics of the diol epoxide derivatives and on the *cis* or *trans* nature of adduct formation. Osborne (1993) modified deoxyribooligonucleotides, about 40 bases long, containing multiple G's, with racemic *anti*-BPDE and observed that these modified oligonucleotides were incompletely digested by SVPD. Cosman (1991) reported a difference in rates of digestion by SVPD of oligonucleotide adducts containing single guanosine residues modified by *trans* addition at the exocyclic amino group by either (+)-*anti*-BPDE or (–)-*anti*-BPDE. In this work, using gel electrophoresis techniques, we show that (–)-*trans* adducts are significantly more resistant to digestion by SVPD than (+)-*trans* adducts, while the opposite order of resistance is observed in the case of digestion with SPD. These differences are related to the steric configurations of these adducts, since the (+)-*trans*- and (–)-*trans*-*anti*-BPDE–oligonucleotide adducts are *chemically* identical (Meehan & Straub, 1979; Cheng et al., 1989). There are two different aspects of these results which are of interest, namely, the identification of the enzyme stall sites, and the differences in the overall rates of digestion of the (+)-*trans*- and (–)-*trans*-oligonucleotide adducts by the same exonuclease.

Stall Sites and Adduct Orientations. The sizes of the most digestion-resistant fragments are summarized in Table I. In the case of the (+)-*trans*-16-mer adduct, the phosphodiester bond most resistant to hydrolysis by both enzymes, SVPD and SPD, is 5′-d(...T-G^{BPDE}...), i.e., is located on the 5′-side of the modified guanosyl residue (the starred G denotes the BPDE-modified G). In contrast, in the case of the (–)-*trans*-

Table I: (+)-*trans*- and (–)-*trans*-BPDE-N^2-dG-Modified 5′-d(CTCACATG*TACACTCT) Oligonucleotides Subjected to Digestion by the Exonucleases SVPD and SPD: Sizes of the Most Enzyme Digestion-Resistant Fragments and Stall Sites

enzyme	digestion	(+)-*trans*-16-mer[a]	(–)-*trans*-16-mer[a]
SVPD	3′ → 5′	5′-d(CTCACAT·*G)	5′-d(CTCACATG*·T)
SPD	5′ → 3′	5′-d(T·*GTACACTCT)#	5′-d(G*·TACACTCT)[b]

[a] The dot between adjacent bases defines the most enzyme digestion-resistant phosphodiester bond. The asterisk (*) indicates the site of BPDE modification. The position of the * symbol on the left- or right-hand sides of the modified G residues denotes the orientation of the pyrenyl ring system toward either the 5′- or the 3′-direction, respectively (see text). [b] The oligonucleotides used in the gel electrophoresis experiments contained an additional ^{32}P-labeled C at the 3′-end.

16-mer adduct, the SVPD and SPD digestion-resistant phosphodiester bond is 5′-d(...G^{BPDE}-T...), i.e., is situated on the 3′-side of the modified G. Thus, while the opposite stereoselectivities are observed in the digestion rates of each of the (+)- and the (–)-*trans* adducts by SVPD or SPD, both enzymes are stalled at the same site in either the (+)-*trans*- or the (–)-*trans* oligonucleotide fragments. These results suggest that, in the (+)-*trans*-oligonucleotide adducts, the pyrenyl ring system is located in the immediate vicinity of the phosphodiester bond on the 5′-side of the modified guanosine, while in the (–)-*trans*-oligonucleotides, the pyrenyl ring system is located near the phosphodiester bond on the 3′-side of the modified single-stranded oligonucleotide.

It is interesting to note that this kind of adduct orientation was determined experimentally in *double-stranded* oligonucleotides from high-resolution 2D NMR studies (Cosman et al., 1992; de los Santos et al., 1992) and was also predicted on the basis of detailed energy-minimization computational studies (Singh et al., 1991). The 2D NMR studies have conclusively shown that in (+)-*trans-anti*-BPDE-N^2-dG oligonucleotide adducts [d(CCATCG^{BPDE}CTACC) sequences] the pyrenyl residues are situated in the minor groove of the duplexes and are oriented toward the 5′-end of the modified strand; in contrast in (–)- *trans-anti*-BPDE-N^2-dG oligonucleotide adducts, the pyrenyl residues tend to be oriented towards the 3′- end of the modified strands (Cosman et al., 1992; de los Santos, et al., 1992). Our own results suggest that similar adduct orientations tend to be maintained even in single-stranded oligonucleotides, since analysis of the enzyme stall sites indicates that the pyrenyl residues are oriented toward the 5′-end in (+)-*trans*-BPDE-N^2-dG oligonucleotide adducts, and towards the 3′-end in the analogous (–)-*trans* adducts. While the sequence context of the modified oligonucleotide used in this work was ...TG^{BPDE}T..., the NMR duplex studies were performed with a ...CG^{BPDE}C... sequence. However, we have observed that the stereoselective enzyme digestion effects are also observed in single-stranded oligonucleotides with a ...CG^{BPDE}C... sequence context (data not shown); therefore, these effects may be general, at least for pyrimidine-G^{BPDE}-pyrimidine sequences.

The stereoselective enzyme digestion results described suggest that these exonuclease digestion methods, coupled with identifications of the enzyme stall sites, can be useful in defining adduct orientations relative to the 5′–3′ strand polarity in single-stranded oligonucleotides containing covalently bound bulky adducts.

The enzyme blocks extend at most one base beyond the BPDE-modified deoxyguanosine either on the 3′-side (in the case of SVPD) or on the 5′-side (in the case of SPD). This corresponds approximately to the geometric dimensions of the pyrenyl ring system which is tilted either toward the 5′-

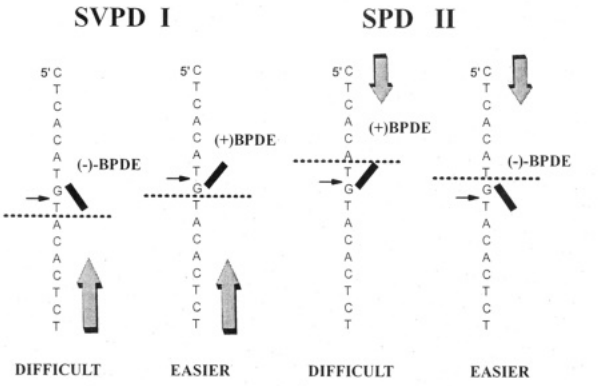

FIGURE 9: Model describing opposite stereoselectivities of enzyme digestion of (+)- and (–)-*trans-anti*-BPDE–oligonucleotide adducts by the exonucleases SVPD and SPD. The dashed horizontal bars define the fragments that are most resistant to enzyme digestion, thus defining the enzyme stall sites (see text). The large vertical arrows indicate the direction of exonuclease digestion, while the small horizontal arrows indicate the most enzyme-resistant phosphodiester bonds.

or the 3′-ends of the modified strands, as found in the NMR studies on duplexes (Cosman et al., 1992; de los Santos et al., 1992). This inhibition of enzyme activities is probably due to a diminished ability of the enzyme to bind to the modified portion of the oligonucleotide, and/or to inhibited hydrolysis at the binding site. The results in Figures 5 and 6 show that at shorter digestion times (1 or 2 min) partially hydrolyzed, longer oligonucleotide fragments are present, but that these fragments are hydrolyzed more rapidly; thus after an additional digestion time (e.g., 30 min, lanes +4 and –9 in Figure 5, or 120 min, lanes +5 and –10 in Figure 6) only the most resistant fragments remain, depending on the enzyme and the enantiomeric BPDE adduct. These results suggest that the activity of the enzymes is also diminished when the BPDE residues are more than one or two bases away from the 5′-OH and 3′-OH termini of the modified oligonucleotides. It should be emphasized that, upon increasing the enzyme concentrations and digestion time, both types of adducts can be completely digested to the mononucleoside levels (as demonstrated by the results shown in Figure 2).

Opposite Stereoselective Resistance to Digestion by the Same Enzyme of (+)-trans- and (–)-trans-Oligonucleotide Adducts. While both enzymes tend to stall at the same sites in either (+)-*trans*- or (–)-*trans*-oligonucleotide adducts, each type of adduct is digested at different rates by SVPD and SPD. This is clearly demonstrated in the case of SVPD in Figure 5, and in the case of SPD in Figure 6. A simple model accounting for the stereoselective, opposite resistance to digestion of these two types of adducts can be proposed on the basis of the orientations of the pyrenyl residues relative to the 5′–3′ strand polarity in (+)-*anti*-BPDE- and (–)-*anti*-BPDE-modified single-stranded oligonucleotides, as discussed above. The salient features of this model are summarized pictorially in Figure 9; the fragments with the greatest resistance to enzyme digestion are denoted by the dashed lines. The small horizontal arrows indicate the the most exonuclease-resistant phosphodiester bonds.

(–)-trans-BPDE-N^2-dG Adducts. With the bulky pyrenyl residues pointing toward the 3′-end, the progress of the SVPD enzyme digestion is impeded by the (-)-BPDE residue which meets it "head-on" as the enzyme progresses from the 3′-end of the modified oligonucleotide toward the 5′-end. According to this model, the progress of the enzyme SPD should be less impeded, since the digestion progresses in the 5′ → 3′ direction,

and the pyrene ring system points into the same direction toward the 3′-end. These predicted relative resistances to enzyme digestion are in agreement with the experimental observations (Figures 5 and 6).

(+)-trans-BPDE-N²-dG Adducts. The above model predicts that the progress of hydrolysis, catalyzed by a given phosphodiesterase, is less impeded when the pyrene ring system points in the same direction as the progression of the enzyme. In (+)-*trans* adducts, the pyrene ring system points toward the 5′-end; it thus follows that SVPD enzyme digestion should be faster in the case of the (+)-*trans*-BPDE adducts than in the case of the (−)-*trans*-BPDE–oligonucleotide adducts, as is indeed observed (Figure 5). This model also predicts that SPD, which hydrolyzes DNA strands in the opposite direction than SVPD, that is, from the 5′- to the 3′-end, should digest the (−)-BPDE adducts faster than the (+)-BPDE adducts. This is indeed observed experimentally (Figure 6), thus supporting the model of relative enzyme digestion activities (Figure 9).

CONCLUSIONS

These observations, though obtained with simple exonucleases, suggest one type of mechanism for explaining differences in the enzymatic processing of (+)-*trans-anti*-BPDE-N²-dG and (−)-*trans-anti*-BPDE-N²-dG lesions in modified DNA. In adducts derived from the covalent binding of these two chiral *anti*-BPDE stereoisomers to DNA, the bulky pyrenyl residues are oriented in different directions relative to the DNA 5′ → 3′ strand polarity, thus affecting the functioning of direction-sensitive enzymes to different extents.

ACKNOWLEDGMENT

We thank Dr. V. Ibanez for synthesizing the 16-mer oligonucleotides. We are grateful to the two reviewers for their important and insightful comments on the manuscript.

REFERENCES

Bernardi, A., & Bernardi, G. (1971) in *The Enzymes* (Boyer, P. D., Ed.) Vol. IV, 3rd ed., pp 329–336, Academic Press, New York.

Brody, R. S. (1991) *Biochemistry 30*, 7072–7080.

Brody, R. S., Doherty, K. G., & Zimmerman, P. D. (1986) *J. Biol. Chem. 261*, 7136–7143.

Brookes, P., & Osborne, M. R. (1982) *Carcinogenesis 3*, 1223–1226.

Buening, M. K., Wislocki, P. G., Levin, W., Yagi, H., Thakker, D. R., Akagi, H., Koreeda, M., Jerina, D. M., & Conney, A. H. (1978) *Proc. Natl. Acad. Sci. U.S.A. 75*, 5358–5361.

Caruthers, M. H. (1982) in *Chemical and Enzymatic Synthesis of Gene Fragments* (Gassen, H. G., & Lang, A., Eds.) pp 71–79, Verlag Chemie, Weinheim.

Cassim, J. Y., & Yang, J. T. (1969) *Biochemistry 8*, 1947–1951.

Cheh, A. M., Yagi, H., & Jerina, D. M. (1990) *Chem. Res. Toxicol. 3*, 545–550.

Cheng, S. C., Hilton, B. D., Roman, J. M., & Dipple, A. (1989) *Chem. Res. Toxicol. 2*, 334–340.

Conney, A. H. (1982) *Cancer Res. 42*, 4875–4917.

Cosman, M. (1991)Ph.D. Thesis, New York University.

Cosman, M., Ibanez, V., Geacintov, N. E., & Harvey, R. G. (1990) *Carcinogenesis 12*, 1667–1672.

Cosman, M., de los Santos, C., Fiala, R., Hingerty, B. E., Ibanez, V., Margulis, L. A., Live, D., Geacintov, N. E., Broyde, S., & Patel, D. J. (1992) *Proc. Natl. Acad. Sci. U.S.A. 89*, 1914–1918.

Cosman, M., de los Santos, C., Fiala, R., Hingerty, B. E., Ibanez, V., Luna, E., Harvey, R. G., Geacintov, N. E., Broyde, S., & Patel, D. (1993) *Biochemistry* (in press).

de los Santos, Cosman, M., Hingerty, B. E., Ibanez, V., Margulis, L. A., Geacintov, N.E., Broyde, S., & Patel, D. J. (1992) *Biochemistry 31*, 5245–5252.

Dipple, A., & Pigott, M. A. (1987) *Carcinogenesis 8*, 491–493.

Geacintov, N. E., Cosman, M., Mao, B., Alfano, A., Ibanez, V., & Harvey, R. G. (1991) *Carcinogenesis 12*, 2099–2108.

Gupta, R. C., Reddy, M. V., & Randerath, K. (1982) *Carcinogenesis 3*, 1081–1092.

Harada, N., & Nakanishi, K. (1983) *Circular Dichroism Spectroscopy. Exciton Coupling in Organic Stereochemistry*, pp 282–285, University Science Books, Mill Valley, CA.

Laskowski, M., Sr. (1971) in *The Enzymes* (Boyer, P. D., Ed.) Vol. IV, 3rd ed., pp 313–328, Academic Press, New York.

Maniatis, T., Fritsch, E. F., & Sambrook, J. (1982) *Molecular Cloning. A Laboratory Manual*, pp 475–478, Cold Spring Harbor Laboratory, Cold Spring Harbor, NY.

Mao, B., Margulis, L. A., Li, B., Ibanez, V., Lee, H., Harvey, R. G., & Geacintov, N. E. (1992) *Chem. Res. Toxicol 5*, 773–778.

Maxam, A. M., & Gilbert, W. (1980) *Methods Enzymol. 65*, 499–560.

McLaughlin, L. W., & Piel, N. (1984) in *Oligonucleotide Synthesis: A Practical Approach* (Gait, M. J., Ed.) pp 117–133, IRL Press, Oxford.

Meehan, T., & Straub, K. (1979) *Nature 277*, 410–412.

Nossal, N. G., & Singer, M. F. (1968) *J. Biol. Chem. 243*, 913–922.

Osborne, M. (1993) *Polycyclic Aromat. Compd. 3* (Supplement), 863–869.

Shibutani, S., Margulis, L. A., Geacintov, N. E., & Grollman, A. P. (1993) *Biochemistry 32*, 7531–7541.

Singer, B., & Grunberger, D. (1983) *Molecular Biology of Mutagens and Carcinogens*, Plenum Press, New York.

Singh, S. S., Hingerty, B. E., Singh, U. C., Greenberg, J. P., Geacintov, N. E., & Broyde, S. (1991) *Cancer Res. 51*, 3482–3492.

Slaga, T. J., Bracken, W. J., Gleason, G., Levin, W., Yagi, H., Jerina, D. M., & Conney, A. H. (1979) *Cancer Res. 39*, 67–71.

Stevens, C. W., Bouck, N., Burgess, J. A., & Fahl, W. E. (1985) *Mutat. Res. 152*, 5–14.

Stezowski, J. J., Loos-Guba, G., Schönwälder, K. H., Straub, A., & Glusker, J. P. (1987) *J. Biomol. Struct. Dyn. 5*, 615–637.

Thomas, K. R., & Olivera, B. M. (1978) *J. Biol. Chem. 253*, 424–429.

Weems, H. B., & Yang, S. K. (1989) *Chirality 1*, 276–283.

Weems, H. B., Fu, P. P., & Yang, S. K. (1986) *Carcinogenesis 7*, 1221–1230.

Wood, A. W., Chang, R. L., Levin, W., Yagi, H., Thakker, D. R., Jerina, D. M., & Conney, A. H. (1977) *Biochem. Biophys. Res. Commun. 77*, 1389–1396.

Yagi, H., Thakker, D. R., Hernandez, O., Koreeda, M., & Jerina, D. M. (1977) *J. Am. Chem. Soc. 99*, 1604–1611.

Yang, S. K., Weems, H. B., Mustaq, M., & Fu, P. P. (1984) *Chromatography 316*, 569–584.